Available online at www.sciencedirect.com
SCIENCE DIRECT
International Journal of Heat and Mass Transfer 49 (2006) 3379–3391
International Journal of HEAT and MASS TRANSFER
www.elsevier.com/locate/ijhmt

Heat transfer from a horizontal fin array by natural convection and radiation—A conjugate analysis

V. Dharma Rao [a,*], S.V. Naidu [a], B. Govinda Rao [b], K.V. Sharma [c]

[a] Department of Chemical Engineering, Andhra University, Visakhapatnam 530 003, India
[b] Department of Mechanical Engineering, G.V.P. College of Engineering, Visakhapatnam, India
[c] Department of Mechanical Engineering, JNTU, Kukatpally, Hyderabad, India

Received 11 April 2005; received in revised form 8 March 2006
Available online 9 June 2006

Abstract

The problem of natural convection heat transfer from a horizontal fin array is theoretically formulated by treating the adjacent internal fins as two-fin enclosures. A conjugate analysis is carried out in which the mass, momentum and energy balance equations for the fluid in the two-fin enclosure are solved together with the heat conduction equations in both the fins. The numerical solutions by using alternating direction implicit (ADI) method yield steady state temperature and velocity fields in the fluid, and temperatures along the fins. Each end fin of the array is exposed to limited enclosure on one side and to infinite fluid medium on the other side. Hence a separate analysis is carried out for the problem of end fin exposed to infinite fluid medium with appropriate boundary conditions. From the numerical results, the heat fluxes from the fins and the base of the two-fin enclosure, and the heat flux from the end fin are calculated. Making use of the heat fluxes the total heat transfer rate and average heat transfer coefficient for a fin array are estimated. Heat transfer by radiation is also considered in the analysis. The results obtained for a four-fin array are compared with the experimental data available in literature, which show good agreement. Numerical results are obtained to study the effectiveness for different values of fin heights, emissivities, number of fins in a fixed base, fin base temperature and fin spacing. The numerical results are subjected to non-linear regression and equations are obtained for heat fluxes from the two-fin enclosure and single fin as functions of Rayleigh number, aspect ratio and fin emissivity. Also regression equations are obtained to readily calculate the average Nusselt number, heat transfer rate and effectiveness for a fin array.

Keywords: Fin array; Natural convection; Radiation; Conjugate problem; Enclosure; Heat transfer

1. Introduction

Extended surfaces, which are popularly known as fins, are extensively used in air-cooled automobile engines and in air-cooled aircraft engines. Fins are also used for the cooling of computer processors, and other electronic devices. Fins are used in the cooling of oil carrying pipe line which runs several hundreds of miles. Heat pipes are also used along with fins to enhance cooling rate. In various applications heat from the fins is dissipated by natural as well as forced convection and radiation. It is observed that radiation contributes up to 20% of the total heat dissipation. Fins are used as arrays in all the applications. The heat transfer rates from fin arrays are found to be lower compared to those predicted theoretically for the case of single fin. The heat transfer rate from the fin array is found to depend on the fin spacing.

There has been continuous research on improving the efficiency of heat exchange systems using fins involving natural convection and forced convection. Early experimental

* Corresponding author. Tel.: +91 891 254 0391.
E-mail addresses: v.dharmarao@yahoo.com (V.D. Rao), svnayudu@yahoo.com (S.V. Naidu), govindarao_budda@rediffmail.com (B.G. Rao), ces_jntu@yahoo.com (K.V. Sharma).

0017-9310/$ - see front matter © 2006 Elsevier Ltd. All rights reserved.
doi:10.1016/j.ijheatmasstransfer.2006.03.010

Nomenclature

A_B	area of the horizontal base plate, (BW), m^2
A_R	aspect ratio for two-fin enclosure, (H/S)
A_w	half the cross-sectional area of the fin, $(t_F W)$, m^2
B	breadth of the horizontal base plate, m
C_p	specific heat, J kg^{-1} K^{-1}
F	radiation shape factor
g	acceleration due to gravity, m s^{-2}
Gr	Grashof number, $g\beta(T_{w,0} - T_\infty)S^3/\nu_f^2$
h	heat transfer coefficient, W m^{-2} K^{-1}
J	radiosity, W m^{-2}
k	thermal conductivity, W m^{-1} K^{-1}
H	height of the fin, m
L^*	characteristic length defined in Eq. (36)
M	fin parameter, $k_f PSGr^{1/4}/(k_w A_w)$
N	number of fins in the fin array
N_R	radiation parameter, $\frac{\sigma T_\infty^4 S}{k_f(T_{w,0}-T_\infty)}\frac{1}{Gr^{1/4}}$
p	pressure, Pascals
P	half-perimeter of the fin, $(2t_F + W)$, m
Pr	Prandtl number, $c_{pf}\mu_f/k_f$
q	heat flux, W m^{-2}
q^+	normalized heat flux, $qS/[k_f(T_{w,0} - T_\infty)]Gr^{1/4}$
Q	heat transfer rate, W
Ra	Rayleigh number, $g\beta(T_{w,0} - T_\infty)S^3/(\nu_f\alpha_w)$
Ra^*	modified Rayleigh number defined in Eq. (36), $g\beta(T_{w,0} - T_\infty)L^{*3}/(\nu_f\alpha_w)$
S	spacing between adjacent fins, m
t_F	half-thickness of the fin, m
t	time, s
t^+	normalized time, $(\nu_f t Gr^{1/2})/S^2$
T	temperature, K
T^+	normalized temperature, $(T - T_\infty)/(T_{w,0} - T_\infty)$
u	velocity component in x-direction, m s^{-1}
u^+	normalized velocity component in x-direction, $Su/(\nu_f Gr^{1/2})$
v	velocity component in y-direction, m s^{-1}
v^+	normalized velocity component in y-direction, $Sv/(\nu_f Gr^{1/4})$
W	width of the fin (also that of base plate), m
x	position coordinate along the fin measured from the base of the fin, m
x^+	normalized position coordinate along the fin, x/S
y	position coordinate normal to the fin measured from the left fin, m
y^+	normalized position coordinate normal to the fin, $yGr^{1/4}/S$

Greek symbols

α	thermal diffusivity of fluid, $(k/\rho c)_f$, m^2 s^{-1}
α^+	α_w/α_f
β	isobaric coefficient or thermal expansion coefficient of fluid, K^{-1}
ε	emissivity
γ	temperature ratio parameter, $(T_{w,0} - T_\infty)/T_\infty$
μ	dynamic viscosity, kg m^{-1} s^{-1}
ν	kinematic viscosity, m^2 s^{-1}
ρ	density, kg m^{-3}
Ψ	stream function
Ψ^+	normalized stream function, $\Psi/(\nu_f Gr^{1/4})$
σ	Stefan–Boltzmann constant, $(5.67 \times 10^{-8}$ W m^{-2} $K^{-4})$
θ_w	T_w/T_∞
ζ	vorticity function, s^{-1}
ζ^+	normalized vorticity function, $S^2\zeta/(\nu_f Gr^{3/4})$

Subscripts

1	fin in a two-fin enclosure
3	base in a two-fin enclosure
5	end fin defined in Eq. (26a)
B	base of the fin array
B, 0	base plate in the absence of fins
E	end fins of the fin array
I	internal fins of the fin array
c	convection
f	fluid
m	average
r	radiation
T	total
w	fin surface
w, 0	base of the fin
∞	ambient medium

work on free convection in horizontal and vertical fin arrays was conducted by Starner and McManus [1], Welling and Wooldridge [2], Harahap and McManus [3], Jones and Smith [4], Donvan and Roher [5], Van de pol and Tierney [6], and Bar-Cohen [7]. Radiation heat transfer plays an important role in heat transfer from fin arrays. Edwards and Chaddock [8] showed that heat transfer by radiation from cylindrical fins of surface emissivity of 0.99 accounted to one-third of the total heat transfer. Chaddock [9] found that heat transfer by radiation from polished aluminum fins was 10–20% of total heat transfer. Sparrow and Acharya [10] presented the article on a natural convection fin with a solution—determined non-monotonically varying heat transfer coefficient. A conjugate conduction–convection analysis has been made for a vertical plate fin which exchanges heat with its fluid environment by natural convection. They showed that the local heat transfer coefficient decreased at first, attained a minimum and then increased with increasing down stream distance. Saikhedkar and Sukhatme [11] observed that convective heat trans-

fer increased and radiative heat transfer decreased with an increase in the Grashoff number. Manzoor et al. [12] analyzed the heat lost from the fins by convection and radiation through one-dimensional and 2D approach. Sparrow and Vemuri [13] conducted experiments on highly populated horizontal pin fins fixed to a vertical base plate. They showed that with fins, heat transfer increased by six times more than the un-finned surface and radiation contribution was 25–40% of the total heat loss. The same authors [14] also studied the effect of orientation of the fin array and heat transfer by radiation was estimated based on isothermal fins. Guglielmini et al. [15] conducted experiments on staggered vertical fins and showed that heat transfer performance of staggered vertical fins is superior to that obtained from fins made up of U-shaped vertical channels of the same bulk volume. Aihara et al. [16] conducted experiments on pin fin arrays with a vertical base plate to study the velocity distributions around pin fin. Radiation was estimated based on the apparent emissivity concept and a formula for apparent emissivity was also presented. According to Zografos and Edward Sunderland [17] a pin fin array performs better than a plate fin array under the same conditions. Sunil Reddy and Sobhan [18] studied the performance of a rectangular fin with a line source at base. The interaction of natural convection with radiation and conduction in a slot was numerically studied by Balaji and Venkateshan [19]. Rao and Venkateshan [20] carried out experiments on horizontal fin arrays. They showed that much larger heat fluxes are in short fins than long fins. Further the convective heat transfer increased linearly with fin spacing, while the increase in radiation heat transfer showed non-linear trend. Lina and Leela [21] applied the second law to a pin fin array under cross flow, and observed that an increase in the cross flow fluid velocity would enhance the heat transfer rate and hence reduce the heat transfer irreversibility. Abramzon [22] presented a discussion on the estimation of radiation heat transfer from rectangular fin arrays, where in radiation contributes 20% of the total heat transfer. Yuncu and Anbar [23] conducted experiments by mounting different numbers of fins on a heated horizontal base plate of width 250 mm. The fin spacing decreased as the number of fins was increased. They found that for a given base-to-ambient temperature difference the convection heat transfer rate from arrays reaches a maximum at a particular fin spacing and fin height. de lieto Vollaro et al. [24] investigated on the optimal configuration of rectangular, vertical fins mounted on a plate. Baskaya et al. [25] solved the three-dimensional elliptic governing equations for horizontal rectangular fin arrays by finite volume based CFD code. They investigated the effects of fin spacing, fin height, length and temperature on performance of rectangular fin arrays. Guvenc and Yuncu [26] carried out an experimental investigation on performance of fin array and found that higher heat transfer enhancement is obtained with vertically oriented base than with horizontally oriented base for fin arrays of same geometry. Chiu and Chen [27] used a Adomain's decomposition procedure to determine the temperature distribution within a convective, radiative longitudinal fin of variable thermal conductivity subject to convection heat transfer. Dayan et al. [28] carried out an experimental and analytical study for a downward-facing hot fin array. They found that the array length, fin spacing and surface temperature effect the heat transfer coefficient mostly compared to the fin height. They also showed that the optimal fin spacing varies within a narrow range that depends primarily on the length of the array. It can be observed that any two adjacent fins in a fin array form a rectangular enclosure. In this context, a theoretical treatment of natural convection heat transfer in enclosures is dealt with by some investigators [29,30] for the cases of non-porous and porous media. The appropriate mass, momentum and energy balance equations for the fluid can be found in these papers.

A survey of literature reveals only a few theoretical studies on horizontal fin arrays. The theoretical study of Baskaya et al. [25] on a horizontal fin array considers natural convection heat transfer only. The radiation mode of heat transfer is not taken into account. Further the computational domain in their paper includes a single fin and half of fin spacing (i.e., $S/2$), thus precluding the adjacent fin or fins. The experimental study of Yuncu and Anbar [23] indicates the effect of the adjacent fins on heat transfer. This point is also revealed by the experimental data of Rao and Venkateshan [20], who found that the heat transfer rate from the end fins is higher compared to that from the internal fins in a four-fin array. These observations prompted the authors to consider the heat transfer to the fluid in a limited enclosure from adjacent fins in a fin array, and also to include radiation mode of heat transfer in their analysis.

Hence the problem of natural convection heat transfer from a horizontal fin array is theoretically tackled by treating the adjacent internal fins as two-fin enclosures. The problem is formulated as a conjugate of convection in the fluid in the enclosure and heat conduction in the fins, and is solved by alternating direction implicit (ADI) method. The case of heat transfer from the end fins is also formulated and solved. From these numerical results the total heat transfer rate from an N-fin array is estimated. Heat transfer by radiation is also considered in the analysis.

2. Physical model and formulation

2.1. Internal fins

The two adjacent internal fins having a common base are shown in Fig. 1(a). The base is maintained at a constant temperature $T_{w,0}$, and $T_{w,0} > T_\infty$, where T_∞ is ambient air temperature. The space between the fins is S. The height and width of each fin are H and W respectively, and the ratio (W/H) is by far greater than unity. The half-thickness of the fin is t_F. Heat is transferred from the fins and the base to the ambient air by convection and radiation.

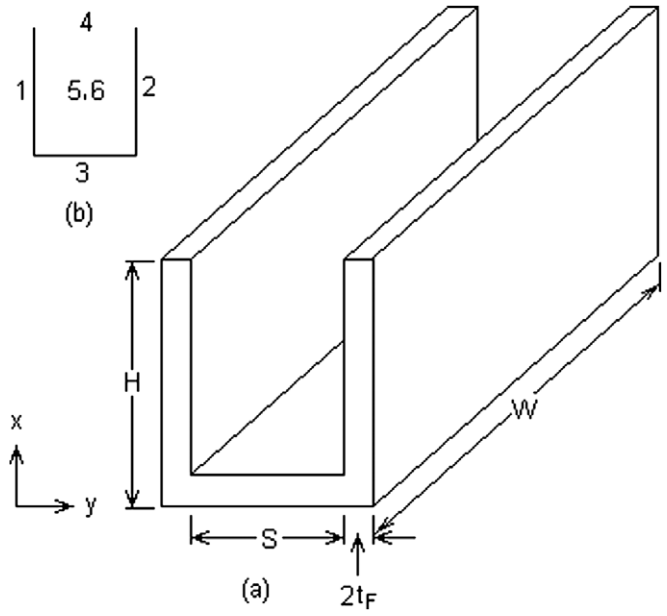

Fig. 1. (a) Physical model of two-fin enclosure. (b) Different surfaces in radiation enclosure.

2.2. Radiation heat transfer

Radiation exchange takes places between the lateral surfaces of fins, the horizontal base and the walls of the room through the top and sides, which are open. For the purpose of radiation heat transfer calculations, the left and right fins and the base are numbered as 1, 2 and 3 respectively as shown in Fig. 1(b). The top, front side and rear side are considered as imaginary surfaces and are numbered 4, 5 and 6 respectively. The radiation passing through these imaginary faces reaches the walls of the room, which is maintained at temperature T_∞. The black body irradiations of the left fin and base are E_{b1} and E_{b3} where $E_{b1} = \sigma T_w^4$ and $E_{b3} = \sigma T_{w,0}^4$. T_w is the temperature of the fin, and $T_w = T_w(x)$. The emissivities of the left fin and the base are ε_1 and ε_3 and the areas are A_1 and A_3 respectively, where $A_1 = HW$ and $A_3 = SW$. The geometric dimensions, properties and temperatures of the left and right fins are identical. Hence $F_{1j} = F_{2j}$ for $j = 1$–6. Further $E_{b1} = E_{b2}$ and $J_1 = J_2$, where J_1 and J_2 are the radiosities. For the imaginary surfaces 5 and 6, $F_{5j} = F_{6j}$ for $j = 1$–6. $E_{b4} = E_{b5} = E_{b6} = J_4 = J_5 = J_6 = \sigma T_\infty^4$. The shape factors F_{12} and F_{31} are computed using the equations available in literature [31]. The shape factors of the remaining surfaces are calculated as follows. $F_{13} = A_3 F_{31}/A_1$, $F_{14} = F_{13}$, $F_{15} = (1 - F_{12} - 2F_{13})/2$, $F_{35} = (1 - 2F_{31} - F_{34})/2$. The following equations can be written for the surfaces 1 and 3 in the radiation network.

$$E_{b1} - J_1 = S_{13}(J_1 - J_3) + (S_{14} + 2S_{15})(J_1 - E_{b4})$$
$$E_{b3} - J_3 = 2S_{31}(J_3 - J_1) + (S_{34} + 2S_{35})(J_3 - E_{b4})$$

where $R_1 = (1 - \varepsilon_1)/\varepsilon_1$; $R_3 = (1 - \varepsilon_3)/\varepsilon_3$; $S_{ij} = R_i F_{ij}$ for any i and j.

The following equations are obtained for J_1 and J_3 from the above equations.

$$J_1 = (a_{22}b_1 + S_{13}b_2)/(a_{11}a_{22} - 2S_{13}S_{31})$$
$$J_3 = (2S_{31}b_1 + a_{11}b_2)/(a_{11}a_{22} - 2S_{13}S_{31}) \quad (1)$$

where $a_{11} = 1 + S_{13} + S_{14}$; $a_{22} = 1 + 2S_{31} + S_{34}$; $b_1 = E_{b1} + S_{14}E_{b4}$; $b_2 = E_{b3} + S_{34}E_{b4}$.

The net radiation heat fluxes q_{r1} and q_{r3} from the fin and the base are as given below.

$$q_{r1} = (E_{b1} - J_1)/R_1 \quad \text{and} \quad q_{r3} = (E_{b3} - J_3)/R_3 \quad (2)$$

2.3. Governing equations

The problem is formulated considering the two vertical fins and the horizontal base together as a two-dimensional enclosure. The two fins and the base are the left, right and bottom boundaries of the enclosure respectively. The top, which is open, is considered to be the fourth boundary. The velocity and temperature fields in the two-fin enclosure are governed by the mass, momentum and energy balance equations for the fluid in conjugation with the one-dimensional heat conduction equation for each fin, which are given below. The radiation components of heat transfer from the fins and the base together are incorporated as a heat generation term in the energy balance equation for the fluid in the enclosure. Thus the equations considered are as follows.

Fluid medium

$$\frac{\partial u}{\partial x} + \frac{\partial v}{\partial y} = 0 \quad (3)$$

$$\rho_f\left(\frac{\partial u}{\partial t} + u\frac{\partial u}{\partial x} + v\frac{\partial u}{\partial y}\right) = -\frac{\partial p}{\partial x} - \rho_f[1 - \beta(T - T_\infty)]g + \mu_f\left(\frac{\partial^2 u}{\partial x^2} + \frac{\partial^2 u}{\partial y^2}\right) \quad (4)$$

$$\rho_f\left(\frac{\partial v}{\partial t} + u\frac{\partial v}{\partial x} + v\frac{\partial v}{\partial y}\right) = -\frac{\partial p}{\partial y} + \mu_f\left(\frac{\partial^2 v}{\partial x^2} + \frac{\partial^2 v}{\partial y^2}\right) \quad (5)$$

$$\rho_f C_{pf}\left(\frac{\partial T}{\partial t} + u\frac{\partial T}{\partial x} + v\frac{\partial T}{\partial y}\right) = k_f\left(\frac{\partial^2 T}{\partial x^2} + \frac{\partial^2 T}{\partial y^2}\right) + q''' \quad (6)$$

where

$$q''' = (2WHq_{r1} + SWq_{r3})/(SWH)$$

where q_{r1} and q_{r3} are given by Eq. (2).

Heat conduction in left fin

$$\rho_w C_{pw}\frac{\partial T_w}{\partial t} = k_w\frac{\partial^2 T_w}{\partial x^2} + \frac{P}{A_w}k_f\frac{\partial T}{\partial y}\bigg|_{y=0} \quad (7)$$

Heat conduction in right fin

$$\rho_w C_{pw}\frac{\partial T_w}{\partial t} = k_w\frac{\partial^2 T_w}{\partial x^2} - \frac{P}{A_w}k_f\frac{\partial T}{\partial y}\bigg|_{y=S} \quad (8)$$

where P and A_w are the half-perimeter and half cross-sectional area of the fin respectively.

$$P = 2t_F + W \quad \text{and} \quad A_w = t_F W$$

The u- and v-momentum balance equations, i.e., Eqs. (4) and (5) are coupled making use of vorticity ζ, which is defined as follows:

$$\zeta = \frac{\partial u}{\partial y} - \frac{\partial v}{\partial x} \tag{9}$$

The terms in Eq. (4) are differentiated with respect to y and those in Eq. (5) are differentiated with respect to x. The resulting equations are subtracted one from the other to yield the following vorticity equation:

$$\rho_f \left(\frac{\partial \zeta}{\partial t} + u \frac{\partial \zeta}{\partial x} + v \frac{\partial \zeta}{\partial y} \right) = \rho_f g \beta \frac{\partial T}{\partial y} + \mu_f \left(\frac{\partial^2 \zeta}{\partial x^2} + \frac{\partial^2 \zeta}{\partial y^2} \right) \tag{10}$$

Thus the problem is governed by the energy balance and vorticity equations, i.e., Eqs. (6) and (10), and the heat conduction equations for fins, i.e., Eqs. (7) and (8).

The stream function ψ is defined as

$$u = \frac{\partial \psi}{\partial y}, \quad v = -\frac{\partial \psi}{\partial x} \tag{11}$$

The vorticity equation in terms of stream function is as follows:

$$\zeta = \frac{\partial^2 \psi}{\partial x^2} + \frac{\partial^2 \psi}{\partial y^2} \tag{12}$$

The stream functions ψ can be evaluated using Eq. (12) if the vorticities ζ are known. The velocity components u and v are to be computed from the values of ψ through Eq. (11).

2.4. Boundary conditions

The boundary conditions at the left, right, bottom and top boundaries of the enclosure are given below.

Left boundary ($y = 0$):

$$T = T_{w,0} = \text{constant at } x = 0 \text{ (fin base)};$$
$$\frac{\partial T}{\partial x} = 0 \text{ at } x = H \text{ (fin tip)}; \quad u = v = \psi = 0 \text{ for } 0 \leqslant x \leqslant H \tag{13}$$

Right boundary ($y = S$):

$$T = T_{w,0} = \text{constant at } x = 0 \text{ (fin base)};$$
$$\frac{\partial T}{\partial x} = 0 \text{ at } x = H \text{ (fin tip)}; \quad u = v = \psi = 0 \text{ for } 0 \leqslant x \leqslant H \tag{14}$$

Base or bottom boundary ($x = 0$):

$$u = v = \psi = 0 \quad \text{and} \quad T = T_{w,0} = \text{constant for } 0 \leqslant y \leqslant S \tag{15}$$

Top boundary at $x = H$:

The top boundary is open, or it is a case of no boundary. Roache [32] described it as an "open flight case" and suggested the following conditions of velocity and temperature to be prescribed on this boundary.

$$v = \frac{\partial u}{\partial x} = \frac{\partial \psi}{\partial x} = \zeta = 0 \quad \text{and} \quad \frac{\partial T}{\partial x} = 0 \tag{16}$$

A discussion on the above boundary condition is given in Roache [32]. There also exist two more alternate conditions that may be used at the top boundary instead of Eq. (16). A discussion on these conditions at the top boundary and their effect on the results is presented in Appendix A.

The values of vorticity ζ at the four boundaries are derived making use of the relevant boundary conditions following Roache [32] and are shown below.

$$\zeta|_{y=0} = \frac{2\psi_{y=\Delta y}}{(\Delta y)^2} \quad \text{for } 0 \leqslant x \leqslant H \text{ (left fin)} \tag{17a}$$

$$\zeta|_{y=S} = \frac{2\psi_{y=S-\Delta y}}{(\Delta y)^2} \quad \text{for } 0 \leqslant x \leqslant H \text{ (right fin)} \tag{17b}$$

$$\zeta|_{x=0} = \frac{2\psi_{x=\Delta x}}{(\Delta x)^2} \quad \text{for } 0 \leqslant y \leqslant S \text{ (base)} \tag{17c}$$

$$\zeta|_{x=H} = 0 \quad \text{for } 0 \leqslant y \leqslant S \text{ (top)} \tag{17d}$$

These boundary conditions for ζ are required for the solution of the vorticity equation. Thus the formulation of the equations and specification of boundary conditions is complete.

All the equations are normalized making use of the following dimensionless variables:

$$x^+ = \frac{x}{S}, \quad y^+ = \frac{y}{S} Gr^{1/4}, \quad t^+ = \frac{\upsilon_f t}{S^2} Gr^{1/2},$$
$$u^+ = \frac{Su}{\upsilon_f} \frac{1}{Gr^{1/2}}, \quad v^+ = \frac{Sv}{\upsilon_f} \frac{1}{Gr^{1/4}}, \quad T^+ = \frac{T - T_\infty}{T_{w,0} - T_\infty},$$
$$\psi^+ = \frac{\psi}{\upsilon_f} \frac{1}{Gr^{1/4}}, \quad \zeta^+ = \frac{S^2 \zeta}{\upsilon_f} \frac{1}{Gr^{3/4}}, \quad \alpha^+ = \frac{\alpha_w}{\alpha_f},$$
$$T_w^+ = \frac{T_w - T_\infty}{T_{w,0} - T_\infty}, \quad E_{b1}^+ = \frac{E_{b1}}{\sigma T_\infty^4} = (\gamma T_{w,1}^+ + 1)^4,$$
$$E_{b3}^+ = (\gamma + 1)^4, \quad E_{b4}^+ = 1,$$
$$q_{ri}^+ = \frac{q_{ri} S}{k_f (T_{w,0} - T_\infty)} \frac{1}{Gr^{1/4}}, \quad J_i^+ = \frac{J_i}{\sigma T_\infty^4}$$

where $i = 1$, 3 and 5. The following are the dimensionless system parameters, namely M, the conduction–convection ratio parameter, N_R, the radiation parameter, A_R, aspect ratio and γ, temperature ratio parameter.

$$M = \frac{k_f P S}{k_w A_w} Gr^{1/4}, \quad N_R = \frac{S \sigma T_\infty^4}{k_f (T_{w,0} - T_\infty)} \frac{1}{Gr^{1/4}},$$
$$A_R = \frac{H}{S}, \quad \gamma = \frac{T_{w,0} - T_\infty}{T_\infty}$$

The energy balance and vorticity equations for the fluid, and heat conduction equations for the left and right fins are shown below in normalized form making use of the dimensionless variables and parameters mentioned above.

$$\frac{\partial T^+}{\partial t^+} + u^+\frac{\partial T^+}{\partial x^+} + v^+\frac{\partial T^+}{\partial y^+} = \frac{1}{Pr}\left(\frac{1}{Gr^{1/2}}\frac{\partial^2 T^+}{\partial x^{+2}} + \frac{\partial^2 T^+}{\partial y^{+2}}\right) + \frac{1}{Pr\,Gr^{1/4}}(2q_{R1}^+ + q_{R3}^+/A_R) \tag{18}$$

$$\frac{Pr\,Gr^{1/2}}{\alpha^+}\frac{\partial T_w^+}{\partial t^+} = \frac{\partial^2 T_w^+}{\partial x^{+2}} + M\left.\frac{\partial T^+}{\partial y^+}\right|_{y^+=0} \tag{19}$$

$$\frac{Pr\,Gr^{1/2}}{\alpha^+}\frac{\partial T_w^+}{\partial t^+} = \frac{\partial^2 T_w^+}{\partial x^{+2}} - M\left.\frac{\partial T^+}{\partial y^+}\right|_{y^+=Gr^{1/4}} \tag{20}$$

$$\frac{\partial \zeta^+}{\partial t^+} + u^+\frac{\partial \zeta^+}{\partial x^+} + v^+\frac{\partial \zeta^+}{\partial y^+} = \frac{\partial T^+}{\partial y^+} + \frac{1}{Gr^{1/2}}\frac{\partial^2 \zeta^+}{\partial x^{+2}} + \frac{\partial^2 \zeta^+}{\partial y^{+2}} \tag{21}$$

The equations defining vortcity and stream function in normalized form are as follows:

$$\zeta^+ = \frac{1}{Gr^{1/2}}\frac{\partial^2 \psi^+}{\partial x^{+2}} + \frac{\partial^2 \psi^+}{\partial y^{+2}} \tag{22}$$

$$u^+ = \frac{\partial \psi^+}{\partial y^+}, \quad v^+ = -\frac{\partial \psi^+}{\partial x^+} \tag{23}$$

The boundary conditions for the inner as well as end fins are also written in normalized form, but are not shown here to conserve space.

3. Method of solution

The procedure used to obtain the temperature and velocity fields as follows. The temperature fields in the two-fin enclosure and on the fins are obtained by the solution of the normalized energy balance equation for the fluid, i.e., Eq. (18) in conjugation with the heat conduction equations for fins, i.e., Eqs. (19) and (20). Alternating direction implicit (ADI) method [32] is used to solve the energy balance equation for the fluid. By this method T^+, the dimensionless temperatures in the fluid are updated in x-direction in the first-half time ($\Delta t^+/2$), and then in y-direction in the second-half time ($\Delta t^+/2$) by solving Eq. (18). Eqs. (19) and (20) are used in the ADI method to update the normalized temperatures on the fins. Subsequently the dimensionless vorticities, ζ^+ at all x^+ and y^+ are updated by solving Eq. (21) using ADI method. The boundary conditions stated in Eqs. (13)–(17) in normalized form are used in the solution of the energy balance and vorticity equations. The solution of these equations yields T^+ and ζ^+ fields at all grid points in the enclosure at each time step, Δt^+. Making use of ζ^+, normalized stream functions ψ^+ are obtained by solving Eq. (22) by successive over relaxation (SOR) method. The normalized velocity components u^+ and v^+ at all x^+ and y^+ (i.e., at all grid points) are calculated by solving Eq. (23). The procedure is continued for successive time steps until steady temperature and velocity fields are obtained at all grid points in the two-fin enclosure.

3.1. Accuracy and convergence criteria

The results by ADI method are obtained choosing a 50×50 uniform grid size corresponding to x- and y-directions respectively. In case of larger S (greater than 20 mm) and larger H (greater than 30 mm) the grid size is increased by 10 on the respective side. It is observed that choosing a sufficiently low time step (Δt^+) is important, particularly during the initial stage when the temperatures on the fins are developing. The following procedure is used to select the time step Δt^+. The ratios $(\Delta x^+)^2/2$ and $(\Delta y^+)^2/2$ are calculated. The minimum of these two $(\Delta t^+)_{min}$ is taken, and Δt^+ is fixed at one-tenth of $(\Delta t^+)_{min}$. A grid-independence test is conducted. Also an independence test is conducted on the value of Δt^+. In computation of the normalized stream functions by successive over relaxation (SOR) method, the values of ψ^+ are improved by means of successive iterations till convergence is obtained within an allowable error equal to 10^{-8}. The error is defined as the absolute value of $(\psi_{ij}^{+(n+1)} - \psi_{ij}^{+(n)})/\psi_{ij}^{+(n)}$, where the superscripts n and $(n+1)$ refer to iteration numbers, and i and j are the grid numbers in x and y directions respectively.

3.2. Heat transfer rate from inner fins and the base

The heat fluxes in dimensionless notation from the left fin and base are given by the following equations:

$$q_1^+ = \frac{1}{A_R}\int_0^{A_R}\left[-\left.\frac{\partial T^+}{\partial y^+}\right|_{y^+=0} + N_R\frac{(E_{b1}^+ - J_1^+)}{R_1}\right]dx^+ \tag{24a}$$

$$q_3^+ = \frac{1}{Gr^{1/4}}\int_0^{Gr^{1/4}}\left[-\frac{1}{Gr^{1/4}}\left.\frac{\partial T^+}{\partial x^+}\right|_{x^+=0} + N_R\frac{(E_{b3}^+ - J_3^+)}{R_3}\right]dy^+ \tag{24b}$$

where E_{b1}^+ and E_{b3}^+ are the black body irradiations in dimensionless form. $E_{b1}^+ = (\gamma T_{w,1}^+ + 1)^4$ and $E_{b3}^+ = (\gamma + 1)^4$. $T_{w,1}^+$ is the normalized fin temperature, which is a function of x^+. γ is the temperature ratio parameter. J_1^+ and J_3^+ are the radiosities in normalized form. The radiosities are to be calculated using the expressions given in Eq. (1). The first and second terms in the above integrals represent the convection and radiation components of the heat fluxes in normalized form. The heat transfer fluxes q_1 and q_3 from the fin and the base are given by the following equations:

$$q_1 = Gr^{1/4}k_f(T_{w,0} - T_\infty)q_1^+/S \tag{25a}$$

$$q_3 = Gr^{1/4}k_f(T_{w,0} - T_\infty)q_3^+/S \tag{25b}$$

It may be noted that q_1 refers to the heat flux from one face of the fin (either left or right) of thickness t_F.

3.3. Heat transfer from the end fins

A separate analysis is carried out to obtain the heat transfer rate from both the end (or, external) fins. This model consists of a fin exposed to an infinite medium of air, which is maintained at a constant temperature T_∞.

In order to use the ADI method, it is considered to be an imaginary enclosure, in which the right boundary is an outflow boundary. Hence $u = \frac{\partial v}{\partial y} = \frac{\partial \psi}{\partial y} = \zeta = 0$. However care is taken in choosing the value of S, which now represents the thickness of the boundary layer. Runs are obtained with $S = 10$, 15 and 20 mm and it is verified that the results do not depend on the value of S. The left boundary, is the fin and hence the boundary condition is the same as Eq. (13). The right boundary is outflow. The same boundary conditions are prescribed at the top boundary as in Eq. (16). For the bottom boundary $u = v = \psi = 0$ and $\frac{\partial T}{\partial x} = 0$. At the bottom $\zeta|_{x=0} = \frac{2\psi_{x=\Delta x}}{(\Delta x)^2}$ and at the top $\zeta|_{x=H} = \frac{2\psi_{x=H-\Delta x}}{(\Delta x)^2}$. The temperatures and vorticities are obtained by solving the energy balance and vorticity equations, Eqs. (18) and (21) using ADI method subject to the boundary conditions for the end fin. Eq. (19) is used to update the temperatures on the fin. The stream functions and velocities are updated with the aid of Eqs. (22) and (23). This procedure is continued at successive time steps until steady state temperature and vorticites are obtained at all grid points.

The dimensionless heat flux from the end fin q_5^+ is given by the following equation in normalized form:

$$q_5^+ = \frac{1}{A_R}\int_0^{A_R}\left[-\left.\frac{\partial T^+}{\partial y^+}\right|_{y^+=0} + \varepsilon_1 N_R\{(\gamma T_w^+ + 1)^4 - 1\}\right] dx^+ \tag{26a}$$

where $\varepsilon_5 = \varepsilon_1$.

The heat flux from the end fin is given by

$$q_5 = Gr^{1/4} k_f (T_{w,0} - T_\infty) q_5^+ / S \tag{26b}$$

Here also it may be noted that q_5 refers to the heat flux from the outer face of the end fin (either first or the last in the array) of half-thickness t_F.

The heat fluxes q_1, q_3 and q_5 for the two-fin enclosure and single fin are computed from the numerical results using Eqs. (24)–(26) respectively. These are further used to calculate the total heat transfer rate, Q_T, the average Nusselt number, Nu_m and effectiveness, E for a fin array containing N fins by the procedure outlined below.

4. Total heat transfer rate from a fin array, Q_T

The breadth of the horizontal base plate, on which the fins are vertically mounted, is given by

$$B = (N-1)S + 2Nt_F \tag{27}$$

where B is the breadth of the plate and N is the number of fins.

The heat transfer rates from the inner fins of the array (Q_I), the base of the fin array (Q_B) and the two end fins (Q_E) are given by

$$Q_I = 2(N-2)H(W + 2t_F)q_1 \tag{28}$$

$$Q_B = (B - 2Nt_F)Wq_3 \tag{29}$$

$$Q_E = 2H(W + 2t_F)(q_1 + q_5) \tag{30}$$

Q_T, the total heat transfer rate from the fin array is given by

$$Q_T = Q_I + Q_B + Q_E \tag{31}$$

4.1. Average Nusselt number for the fin array, Nu_m

Total heat transfer area for the N-fin array is given by

$$A_T = (B - 2Nt_F)W + 2NH(W + 2t_F) \tag{32}$$

The average heat transfer coefficient, h_m for the N-fin array for combined convection and radiation is defined by the following equation:

$$h_m = \frac{Q_T}{A_T(T_{w,0} - T_\infty)} \tag{33}$$

The average Nusselt number for the N-fin array is defined as

$$Nu_m = h_m S / k_f \tag{34}$$

4.2. Effectiveness of the fin array, E

The effectiveness of the fin array is defined as the ratio of heat transfer with fins to that without fins over the same area of the base plate of breadth B and width W. The area of the base plate is given by

$$A_B = BW \tag{35}$$

$Q_{B,0}$, the heat transfer rate from the base plate in the absence of fins is calculated as follows. The Nusselt number for natural convection heat transfer from the horizontal plate is calculated using the equation available in literature [31] as follows:

$$\frac{h_{B,0}L^*}{k_f} = 0.54Ra^{*0.25} \tag{36}$$

where $Ra^* = g\beta(T_{w,0} - T_\infty)L^{*3}/(\nu_f \alpha_f)$ and $L^* = A_B/\{2(B + W)\}$. The equation shown above is valid in the range $10^4 \leqslant Ra^* \leqslant 10^7$.

$Q_{B,0}$, the heat transfer rate from the horizontal plate by convection and radiation is

$$Q_{B,0} = A_B[h_{B,0}(T_{w,0} - T_\infty) + \varepsilon_3\sigma(T_{w,0}^4 - T_\infty^4)] \tag{37}$$

Thus the effectiveness of the fin array is

$$E = Q_T / Q_{B,0} \tag{38}$$

5. Results and discussion

Validation of the present theoretical model is made by a comparison with the experimental data of four different references available in literature. Experimental data of Rao and Venkateshan [20] for a four-fin array are shown in Fig. 2 for two different fin emissivities, viz., $\varepsilon_1 = 0.05$ and $\varepsilon_1 = 0.85$. The experimental data of Jones and Smith [4] are also shown in Fig. 2. Numerical results are obtained

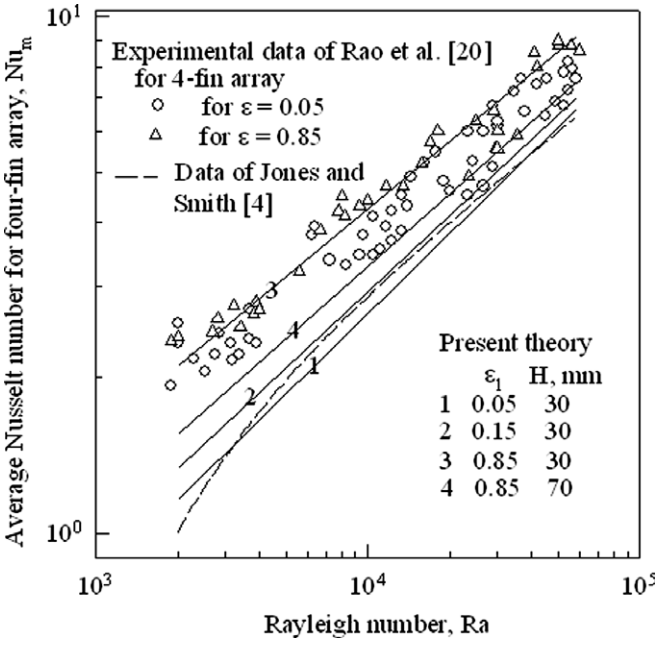

Fig. 2. Comparison of the present theoretical results with the experimental data.

for $S = 10$, 15, 20 and 25 mm, for $H = 30$ and 70 mm, for $\varepsilon_1 = 0.05$, 0.15 and 0.85, and for $T_{w,0} = 60$, 70, 80, 90 and 104 °C. The properties and other data used are as follows: $k_w = 205\ \mathrm{W\ m^{-1}\ K^{-1}}$, $\varepsilon_3 = 0.85$, $t_F = 0.75$ mm, $W = 50$ mm, $T_\infty = 31$ °C. Average Nusselt numbers for a four-fin array ($N = 4$) are computed using Eqs. (28)–(34). Since there are a good number of theoretical points, the points are not shown to avoid cluster and only the lines passing through the points are shown. It is observed from Fig. 2 that at low fin emissivities, i.e., at $\varepsilon_1 = 0.05$ and 0.15 the numerical results agree well with Jones and Smith [4]. At low fin heights ($H = 30$ mm) and high emissivities such as $\varepsilon_1 = 0.85$ the numerical results from the present theory agree well with Rao and Venkateshan [20]. The average Nusselt numbers computed from the present theory show the same orders of magnitude as the experimental data shown in Fig. 2. The contributions of the inner fins, total base and end fins to the total heat transfer is examined from the computer run for $H = 70$ mm, $T_{w,0} = 108.4$ °C, $S = 25$ mm, $\varepsilon_1 = \varepsilon_3 = \varepsilon_5 = 0.85$. It is observed from the numerical results that these contributions are 7.74 W (36.0%), 2.90 W (13.5%) and 10.97 W (50.5%) respectively. These results are sufficiently close to the experimental observations of Rao and Venkateshan [20].

Certain representative numerical results are presented in Table 1, which illustrate the effect of fin spacing (S) on heat transfer fluxes in a two-fin enclosure and on heat transfer rates from a fin array. The heat fluxes from fin (q_1) and that from base (q_3) are obtained from the numerical solution of the equations for a two-fin enclosure. The heat flux from end fin (q_5) is obtained from the analysis for a single fin. Making use of these values of q_1, q_3 and q_5, the heat flow rates Q_I (internal fins), Q_B (base) and Q_E (end fins) for a fin array are calculated using Eqs. (28)–(30). The values of Q_T (total heat transfer rate), h_m (mean heat transfer coefficient) and E (effectiveness) are calculated from Eqs. (31), (33) and (38) respectively. The values of the fin spacing (S) are selected in such a way that all results presented in Table 1 are for a fin array base of the same breadth, i.e., $B = 66$ mm. This facilitates comparison of performance of arrays of different number of fins over a fixed base. It can be observed that with an increase in the number of fins from 4 to 16 the value of S decreases from 20 to 2.8 mm. The heat fluxes from fin (q_1) and that from base (q_3) decrease from 149 to 44 W m^{-2}, and from 379 to 148 W m^{-2} respectively. Even though the number of fins is increased from 4 to 16, the heat transfer rate and effectiveness do not change appreciably. However there is sharp decrease in the average heat transfer coefficient of the fin array (h_m) from 5.29 to 1.48 W m^{-2} K^{-1}.

Yuncu and Anbar [23] obtained experimental data for a fin array to study the effect of increasing the number of fins on heat transfer rate from internal fins, i.e., Q_I, which is defined in Eq. (28). It can be observed from Eq. (27) that for a fixed base (B), as the number of fins increases, the fin spacing decreases. The experimental data of Yuncu and Anbar [23] are shown plotted in Fig. 3. They found that as the number of fins on a horizontal plate is increased, Q_I increased and reached a maximum. However when the number of fins is increased further, the fin spacing becomes very low, and Q_I starts decreasing. A comparison with the experimental observation of Yuncu and Anbar [23] is shown in Fig. 3. Numerical results are obtained for this purpose for a fin array with a base of 250 mm

Table 1
(i) Effect of fin spacing S on heat fluxes q_1 and q_3 for a two-fin enclosure, and (ii) effect of number of fins on Q_T, E and h_m for fin-array for $B = 66$ mm

Two-fin enclosure, $Q_5 = 253$ W m^{-2}				Fin array, $B = 66$ mm, $(Q_{B,0}/A_B) = 255$ W m^{-2}, $S = (B - 2Nt_F)/(N - 1)$			
S, mm	Ra	q_1, W m^{-2}	q_3, W m^{-2}	N	Q_T, W	E	h_m, W m^{-2} K^{-1}
$H = 30$ mm, $T_{w,0} = 70$ °C, $t_F = 0.75$ mm							
20.0	20,371	149	379	4	3.24	3.84	5.29
11.4	3773	96	214	6	2.83	3.35	3.31
7.7	1163	71	194	8	2.78	3.30	2.54
4.4	217	55	168	12	2.98	3.50	1.89
2.8	56	44	148	16	3.04	3.61	1.48

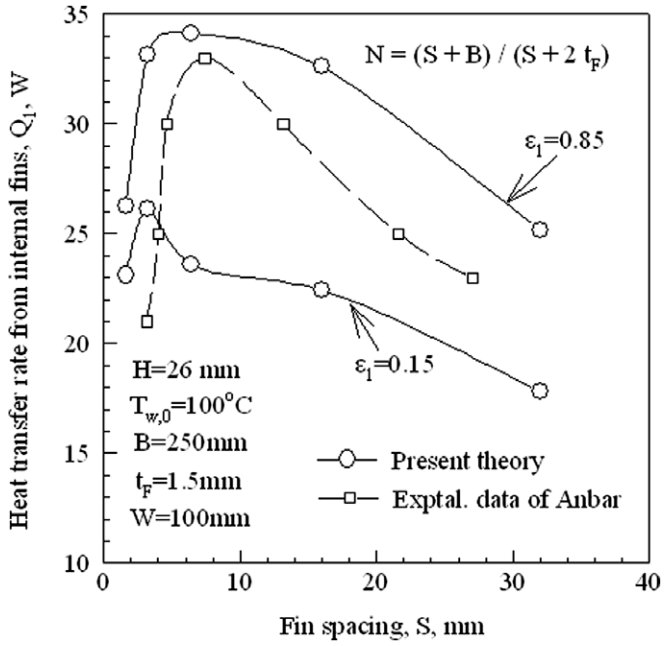

Fig. 3. Heat transfer from internal fins in a fin array—effect of increasing the number of fins on Q_1.

and 8 fins mounted on it. The number of fins on the same base is increased to 14, 27, 41 and 55, and results are obtained for each case. Computer results are obtained for the two-fin enclosure with each value of S. The common parameters chosen are: $H = 26$ mm, $T_{w,0} = 100$ °C, $W = 100$ mm, $t_F = 1.5$ mm, $T_\infty = 31$ °C and $\varepsilon_3 = 0.85$. Since the emissivity of fin in the experiment of Yuncu and Anbar [23] is not mentioned in their paper, numerical results are obtained for two-fin emissivities, viz., $\varepsilon_1 = 0.15$ and 0.85. From the results for each S, the effectiveness is calculated using Eqs. (27)–(38). The results are shown in Fig. 3 for Q_I as a function of S. It is observed that with a decrease in fin spacing, there is an increase in Q_I, which is due to the increase in the number of fins and a corresponding increase in the heat transfer area provided by fins. However when the number of fins is increased beyond a certain value (say 41), a decrease in Q_1 is observed due to very low value of S. The reason for this decrease may be attributed to excessive heating of the fluid in the fin enclosure resulting in a decreased thermal potential. It can be observed from Fig. 3 that the data of Yuncu and Anbar [23] between the numerical results for $\varepsilon_1 = 0.15$ and 0.85.

Starner and McManus, Jr. [1] reported experimental results with $H = 12.7$ mm, $W = 254$ mm, $t_F = 0.508$ mm, $S = 6.35$ mm and $N = 17$. Their calculations consider convection only, thus precluding any radiation heat transfer. Numerical results are obtained for three values of $T_{w,0}$ such as 86, 126 and 196 °C. For these three values of $T_{w,0}$, the average convection heat transfer coefficients (viz., excluding radiation heat flux) are calculated, which are 2.3, 2.5 and 2.9 W m^{-2} K^{-1} respectively. For the values of the above system parameters, Starner and McManus, Jr. [1] reported the experimental average heat transfer coefficients as 1.59, 2.27 and 2.83 W m^{-2} K^{-1} respectively.

Fig. 4 and Table 2 show the effects of fin base temperature ($T_{w,0}$), fin spacing (S) and fin height (H) on total heat transfer rate (Q_T) and effectiveness (E) of fin array. Fig. 4 indicates that Q_T increases as $T_{w,0}$ increases for all S and H. However at a low value of S, i.e., at $S = 5$ mm, the effectiveness (E) is found to decrease with an increases in $T_{w,0}$. This is due to the fact that at a low value of S the rate of increase in Q_T with an increase in $T_{w,0}$ is less compared to the increase in $Q_{B,0}$ with an increase in $T_{w,0}$. $Q_{B,0}$ is the heat flow rate from the base in the absence of fins. In Table 2, the values Q_T and E are shown as functions of $T_{w,0}$ and S. Table 2 also shows the values of Q_I, Q_B and Q_E as functions of $T_{w,0}$ and S. Fig. 4 shows a clear increase in both Q_T and E with an increase in the fin height (H). The increase in Q_T and E with an increase in H is due to the increase in the heat transfer rate from both the internal and end fins (Q_I and Q_E), as can be observed from Table 2.

The half-thickness of fin (t_F) and the thermal conductivity of the fin material (k_w) appear in the fin parameter (M), which is also called as convection-to-conduction ratio parameter. As M tends to zero the fin tends to an isothermal plate. Hence the heat transfer rate from the fin increases, as the value of M decreases. Numerical results are obtained to study the effect of thickness of fin on the heat flux from the fin (q_1). Computer runs for the case of a two-fin enclosure are obtained at $S = 20$ mm, $T_{w,0} = 70$ °C, $k_w = 205$ W m^{-1} K^{-1} and $H = 30$ mm. It is observed that for values of t_F equal to 0.75 and 3.0 mm, the values of q_1 are 148.6 and 150.6 W m^{-2} respectively, thus indicating negligible change only in q_1 due to low height and high thermal conductivity of the fin. However

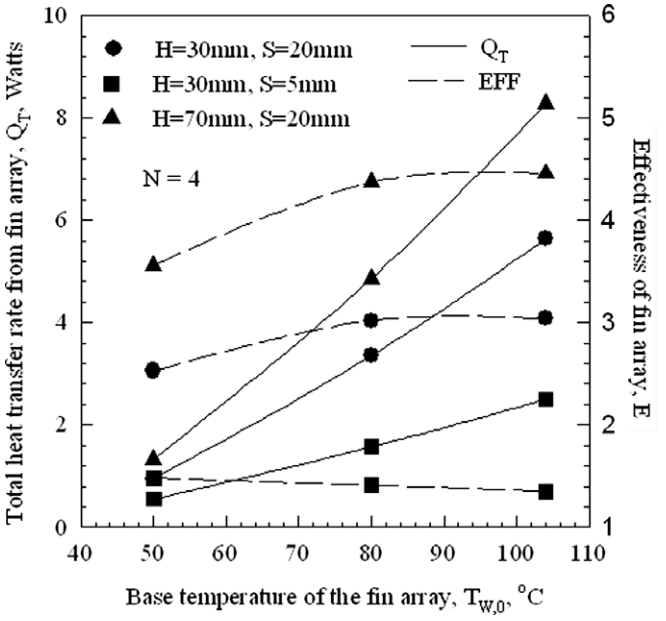

Fig. 4. Effect of base temperature on total heat transfer rate (Q_T) and effectiveness (E) of a four-fin array.

Table 2
Effects of fin base temperature ($T_{w,0}$), fin spacing (S) and fin height (H) on (i) heat fluxes in a two-fin enclosure, and (ii) total heat transfer rate (Q_T) and effectiveness (E) of fin array

$T_{w,0}$ °C	Two-fin enclosure			Four-fin array				
	q_1, W m^{-2}	q_3, W m^{-2}	q_5, W m^{-2}	Q_I, W	Q_B, W	Q_E, W	Q_T, W	E
$H = 30$ mm, $S = 20$ mm								
50	53	57	99	0.32	0.17	0.46	0.95	2.53
80	187	239	318	1.12	0.72	1.51	3.35	3.02
104	316	413	516	1.90	1.24	2.50	5.64	3.04
$H = 30$ mm, $S = 5$ mm								
50	22	4.50	111	0.14	0.01	0.40	0.55	1.48
80	64	13.4	319	0.38	0.04	1.15	1.57	1.41
104	102	22.4	505	0.61	0.07	1.82	2.50	1.35
$H = 70$ mm, $S = 20$ mm								
50	34	17	79	0.48	0.05	0.79	1.32	3.56
80	136	82	251	1.90	0.25	2.71	4.86	4.37
104	239	141	405	3.34	0.42	4.51	8.27	4.46

at a higher value of H, i.e., at $H = 70$ mm and $t_F = 3.0$ mm, with the other parameters remaining the same, q_1 is found to be 101.2 W m^{-2}. The effect of k_w, the thermal conductivity of the fin is also studied. The fin heat flux, $q_1 = 138.4$ W m^{-2} at $k_w = 40$ W m^{-1} K^{-1}, $t_F = 0.75$ mm and $H = 30$ mm, with the other parameters remaining as stated above. Thus the fin effect (i.e., decrease in q_1) is found with a decrease in k_w even for shorter fins. An increase in emissivity of the fin material from 0.05 to 0.85 increases the radiation component of heat transfer from the fin, thus resulting in an increase in the total heat transfer rate from the fin by convection and radiation.

An important outcome of the present theoretical investigation is that it provides the temperatures and velocities at all positions in the enclosure, from which the nature of their variation in the enclosure can be known for different choices of the system parameters. As an example, the effect of the fin spacing on the temperature and velocity profiles of the fluid in the two-fin enclosure are shown in Figs. 5 and 6 respectively. The results shown in these figures correspond to $H = 70$ mm and $T_{w,0} = 104$ °C. In each figure the profiles are shown for two values of fin spacing, namely for $S = 10$ mm and $S = 25$ mm by continuous and broken lines respectively. For each S the profiles are shown at three different heights, viz., $x = H/4$, $x = H/2$ and $x = H$. A comparison of the temperature profiles in Fig. 5 at $S = 10$ mm and at $S = 25$ mm indicates that the temperature far away from the fins (or near $y = S/2$) is lower at $S = 25$ mm compared to that at $S = 10$ mm. However it can be found from Fig. 6 that there is a greater recirculation of the fluid at larger S, resulting in at higher velocities near the wall and lower velocities at mid-spacing ($y = S/2$).

Isotherms and streamlines are shown in Fig. 7 from computer results obtained at $H = 70$ mm and $T_{w,0} = 104$ °C for two different values of fin spacing, S, viz., $S = 10$ mm and 25 mm. The sub-figures (a) and (b) in Fig. 7 show isotherms in the two-fin enclosure for $S = 10$ and 25 mm respectively. The vertical axes on the left and

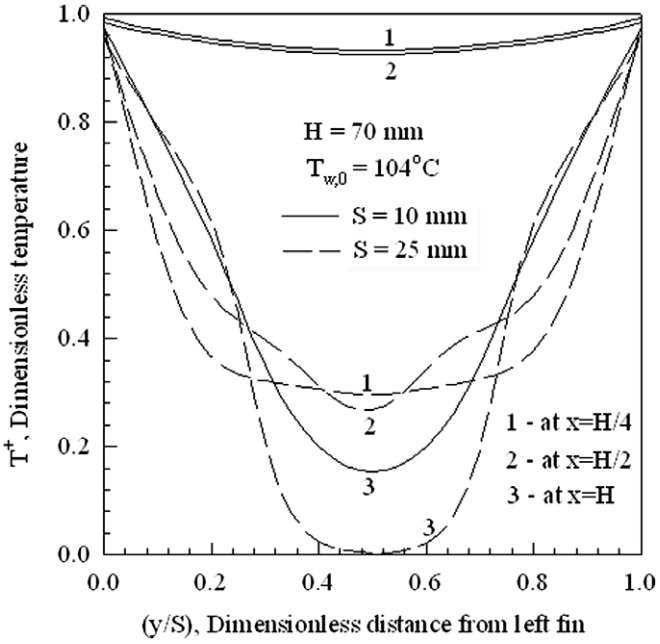

Fig. 5. Temperature profiles for fluid in two-fin enclosure—effect of fin spacing.

right of the enclosure represent the left and right fins respectively. The horizontal axis at the bottom represents the fin base. The isotherms in the sub-figures (a) as well as (b) are shown at 13 different values of dimensionless temperature, viz., $T^+ = 0.02$, 0.05, 0.1, 0.2, 0.3, 0.4, 0.5, 0.6, 0.7, 0.8, 0.9, 0.95 and 0.98. In Fig. 7(a), the first and third isotherms counted from the bottom, at $T^+ = 0.98$ and 0.90 respectively are shown by arrows. A comparison of sub-figures (a) and (b) indicates that at $S = 10$ mm the temperature of air in the middle of the enclosure is heated to a high temperature, and at $S = 25$ mm the heating is confined to the air near the fins and base only. This fact can be observed from a comparison of the isotherms for $T^+ = 0.4$ through 0.9 in sub-figures (a) and (b) of Fig. 7.

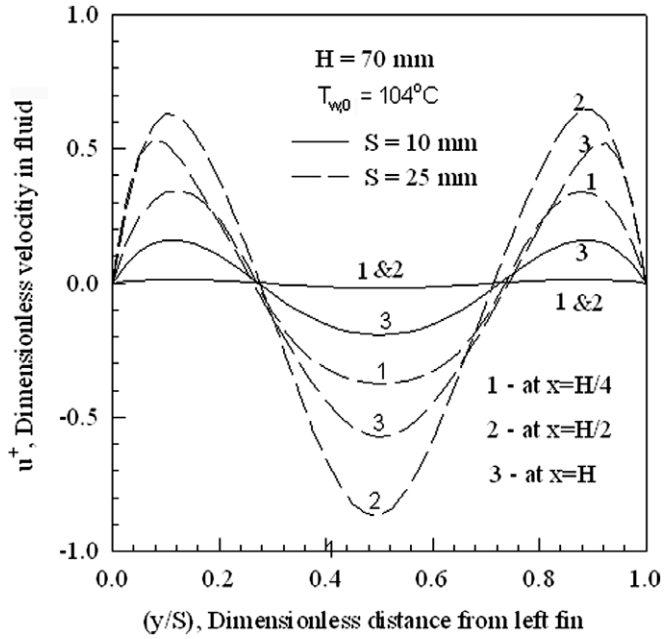

Fig. 6. Velocity profiles for fluid in two-fin enclosure at different heights—effect of fin spacing.

These isotherms are nearer to the top of the enclosure in sub-figure (a), while they lie near to the bottom or base in sub-figure (b).

The streamlines for $S = 10$ and 25 mm are shown in the sub-figures (c) and (d) of Fig. 7 respectively. It is found that for $S = 10$ mm, φ^+ varies from -0.257 to $+0.257$. When $S = 25$ mm, φ^+ lies between -2.0 and $+2.0$. Streamlines are shown in sub-figure (c) for 13 selected values of $-\varphi^+$ and another 13 values of $+\varphi^+$. These values of φ^+ are picked as $(-a\varphi^+_{max})$ and $(a\varphi^+_{max})$, for $a = 0.02$, 0.05, 0.1, 0.2, 0.3, 0.4, 0.5, 0.6, 0.7, 0.8, 0.9, 0.95, and 0.98, where $\varphi^+_{max} = 0.257$. In sub-figure (d) also the values of φ^+ are selected in the same way for $\varphi^+_{max} = 2.0$. It can be observed that the streamlines in the left and right halves are almost symmetric. However φ^+ is positive in the left half, while it is negative in the right half of the enclosure. It can be found from either of these sub-figures that the streamlines travel upwards along the left and right walls or fins, where the temperature is high compared that of the air in the enclosure. When $S = 25$ mm, recirculation of air in the middle of the enclosure can be found, which is shown in the sub-figure (d) of Fig. 7.

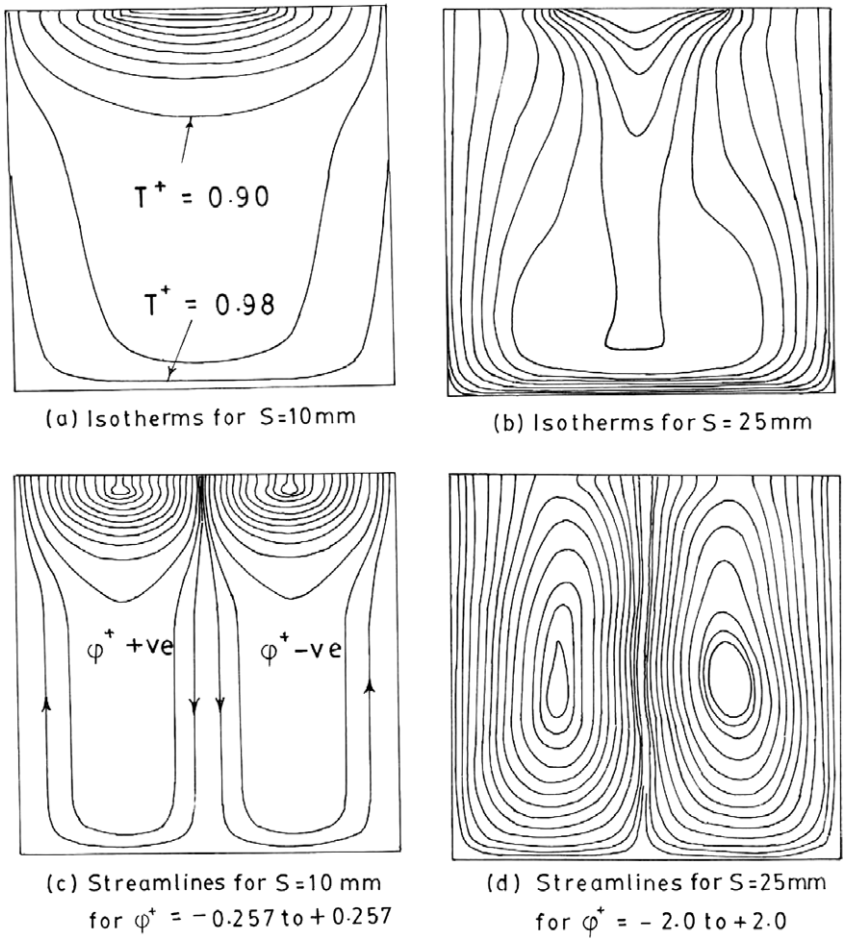

Fig. 7. Isotherms and streamlines for the fluid in the two-fin enclosure at $H = 70$ mm, and $T_{w,0} = 104$ °C—effect of fin spacing for $S = 10$ and 25 mm.

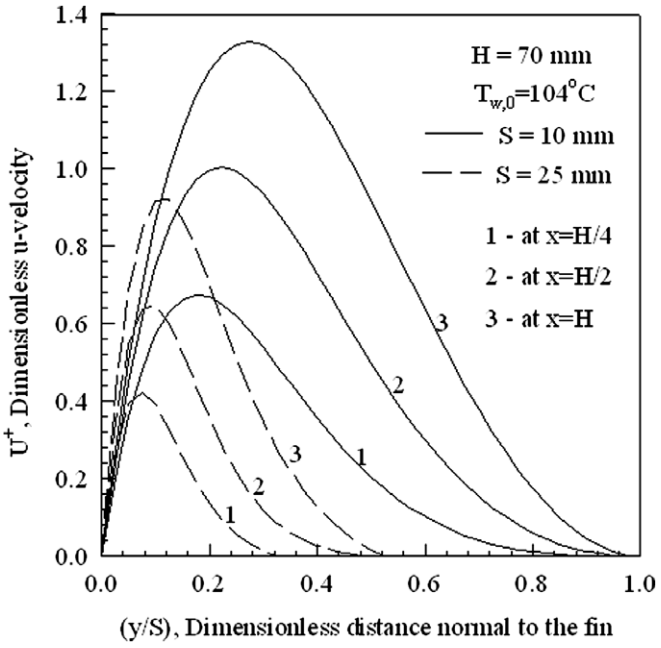

Fig. 8. Velocity profiles for end fin at different heights in the enclosure $S = 10$ mm and $S = 25$ mm.

The velocity profiles for the case of the single fin (end fin) exposed to large ambient medium are shown in Fig. 8 for two values of fin spacing, i.e., for $S = 10$ mm (continuous lines) and for $S = 25$ mm (broken lines).

5.1. Regression equations

The usefulness of the heat fluxes q_1, q_3 and q_5 is evident that they can be used to calculate Q_T, Nu_m and E for a fin array. Hence the following equations are obtained for q_1, q_3 and q_5 as functions of system parameters by performing non-linear regression on the numerical results.

$$\frac{q_1 S}{k_f(T_{w,0}-T_\infty)} = 0.047 Ra^{0.42}\left(\frac{S}{H}\right)^{0.4}\left(\frac{1+\varepsilon_1}{1+N_R}\right)^{0.022} \quad (39)$$

$$\frac{q_3 S}{k_f(T_{w,0}-T_\infty)} = 0.023 Ra^{0.55}\left(\frac{S}{H}\right)^{1.32}\left(\frac{1+\varepsilon_3}{1+N_R}\right)^{0.087} \quad (40)$$

$$\frac{q_5 S}{k_f(T_{w,0}-T_\infty)} = 0.52 Ra^{0.23}\left(\frac{S}{H}\right)^{0.29}\left(\frac{1+\varepsilon_1}{1+N_R}\right)^{0.42} \quad (41)$$

Eqs. (39)–(41) predict the numerical results within a standard deviation of ±6.1% for the range of parameters: $10 \leqslant S \leqslant 25$ mm, $60 \leqslant T_{w,0} \leqslant 104$ °C, $30 \leqslant H \leqslant 70$ mm, $2300 \leqslant Ra \leqslant 60{,}000$, $0.05 \leqslant \varepsilon_1 \leqslant 0.85$, and $0.3 \leqslant N_R \leqslant 1$. Also from the numerical results, the values of Q_T, Nu_m, and E are generated for different sets of fins such as $N = 4$, 8, 16 and 32 making use of Eqs. (31), (34) and (38). Using these values regression equations are obtained for heat transfer rate, average Nusselt number and effectiveness for an N-fin array.

$$Nu_m = 0.102 Ra^{0.36}\left(\frac{S}{H}\right)^{0.4}\left(\frac{1+\varepsilon_1}{1+N_R}\right)^{0.1} N^{-0.04} \quad (42)$$

$$E = 0.022 Ra^{0.33}\left(\frac{S}{H}\right)^{-0.41}\left(\frac{1+\varepsilon_1}{1+N_R}\right)^{-0.16} N^{0.9} \quad (43)$$

Since $Nu_m = \frac{(Q_T/A_T)S}{k_f(T_{w,0}-T_\infty)}$, Eq. (42) can be used to obtain Q_T as well. Eqs. (42) and (43) agree with the numerical results within a standard deviation of ±3.3% for the range of parameters mentioned above.

6. Conclusions

1. A theoretical model is postulated to tackle the problem of heat transfer from a horizontal fin array. According to the model, the fin array is assumed to be formed by joining successive two-fin enclosures. The problem for the case of a two-fin enclosure is theoretically formulated and solved considering heat transfer by natural convection and radiation. The problem for the case of a single fin is also formulated and solved to account for the heat loss from end fins in the array.
2. Making use of the numerical results for the two-fin enclosure and those for the single fin, a procedure is outlined to assess the total heat transfer rate, average Nusselt number and effectiveness for a fin array. The effect of the system parameters, such as fin spacing, number of fins, fin height, fin base temperature is studied on the total heat transfer from the fin array.
3. A comparison with the experimental data existing in literature indicates satisfactory agreement.
4. Numerical results are presented in the figures and tables for the heat fluxes from the fin and base (q_1 and q_3) in the two-fin enclosure, and the heat transfer rates from internal fins (Q_I), base (Q_B) and end fins (Q_E) as functions of the system parameters such as $T_{w,0}$, S and H.
5. Regression equations are presented from the numerical results for the heat fluxes from inner fin and base in the two-fin enclosure and for the heat flux from the end fin. Also regression equations are obtained for the average Nusselt number of the fin array as functions of system parameters.

Appendix A

A.1. Effect of the condition prescribed at top boundary

A topic of theoretical interest, viz., the effect of the condition prescribed at the top boundary on the numerical results is discussed. The top boundary is open or it can be said that there is no top boundary. However as per the requirement in ADI method values have to be prescribed for velocities and temperatures or their first derivatives at the top boundary also on par with the other boundaries. The conditions chosen in the present analysis are given in Eq. (16). In Eq. (16) the temperature derivative is set equal to zero. As another possibility, one can prescribe the temperature at T_∞, the ambient temperature, as shown below.

$$v = \frac{\partial u}{\partial x} = \frac{\partial \psi}{\partial x} = \zeta = 0 \quad \text{and} \quad T = T_\infty \tag{16a}$$

Further in Eq. (16) the velocity component u is not made zero, and hence $\partial u/\partial x = 0$ from the equation of continuity. The following two possible conditions emanate, if the condition that $u = 0$ is used at the top boundary.

$$u = v = \psi = 0, \quad \text{and} \quad \frac{\partial T}{\partial x} = 0 \text{ for } 0 \leqslant y \leqslant S \tag{16b}$$

$$u = v = \psi = 0, \quad \text{and} \quad T = T_\infty \text{ for } 0 \leqslant y \leqslant S \tag{16c}$$

The boundary conditions given by Eqs. (16b) and (16c) were used in literature for the cases of both open and closed top boundaries. Numerical results are obtained making use of the above three conditions also, but are not shown here to conserve space. It is observed that slightly higher Nusselt numbers are obtained particularly at low values of S with the boundary condition given by Eq. (16a) compared to the results obtained using Eq. (16). An optimum fin spacing does not appear if the condition of $T = T_\infty$ from Eq. (16a) is implemented at the top boundary.

References

[1] K.E. Starner, H.N. McManus Jr., An experimental investigation of free convection heat transfer from rectangular fin arrays, J. Heat Transfer 85 (1963) 273–278.

[2] J.R. Welling, C.V. Wooldridge, Free convection heat transfer coefficients from rectangular fin arrays, ASME J. Heat Transfer 87 (1965) 439–444.

[3] F. Harahap, H.N. McManus, Natural convection heat transfer from horizontal rectangular fin arrays, ASME J. Heat Transfer 89 (1967) 32–38.

[4] Charles D. Jones, Lester F. Smith, Optimum arrangement of rectangular fins on horizontal surfaces for free convection heat transfer, ASME J. Heat Transfer 92 (1970) 6–10.

[5] R.C. Donvan, W.M. Roher, Radiative and convective conducting fins on a plane wall, including mutual irradiation, ASME J. Heat Transfer 93 (1971) 41–46.

[6] D.W. Van de pol, J.K. Tierney, Free convective heat transfer from vertical fin arrays, IEEE Trans. PHP-10 (4) (1974) 267–271.

[7] A. Bar-Cohen, Fin thickness for an optimized natural convection array of rectangular fins, Trans. ASME 101 (1979) 564–566.

[8] J.A. Edwards, J.B. Chaddock, An experimental investigation of the radiation and free convection heat transfer from a cylindrical disk extended surface, Trans. Am. Soc. Heat. Refrig. Air-condit. Eng. 69 (1963) 313–322.

[9] J.B. Chaddock, Freeconvection heat transfer from vertical fin arrays, ASHRAE J. 12 (1970) 53–60.

[10] E.M. Sparrow, S. Acharya, A natural convection fin with a solution—determined nonmonotonically varying heat transfer coefficient, ASME J. Heat Transfer 105 (1981) 218–225.

[11] N.H. Saikhedkar, S.P. Sukhatme, Heat transfer from rectangular cross-sectioned vertical fin arrays, in: Proceedings of the sixth national heat and mass transfer conference, HMT, 1981, pp. 9–81.

[12] M. Manzoor, D.B. Inham, P.J. Heggs, The one dimensional analysis of fin assembly heat transfer, ASME J. Heat Transfer 105 (1983) 645–651.

[13] E.M. Sparrow, S.B. Vemuri, Natural convection–radiation heat transfer from highly populated pin –fin arrays, ASME J. Heat Transfer 107 (1985) 190–197.

[14] E.M. Sparrow, S.B. Vemuri, Orientation effects on natural convective/radiation pin-fin arrays, Int. J. Heat Mass Transfer 29 (1986) 359–368.

[15] G. Guglielmini, E. Nannel, G. Tanda, Natural convection and radiation heat transfer from staggered vertical fins, Int. J. Heat Mass Transfer 30 (1987) 1941–1948.

[16] T. Aihara, S. Maruyama, S. Kobayakawa, Free convective–radiative heat transfer from pin-fin arrays with a vertical base plate, Int. J. Heat Mass Transfer 33 (1990) 1223–1232.

[17] Antonios I. Zografos, J. Edward Sunderland, Natural convection from pin fin arrays, Exp. Therm. Fluid Sci. 3 (1990) 440–449.

[18] J.R.N.S. Sunil Reddy, C.B. Sobhan, Natural convection heat transfer from a thin rectangular fin with a live source at the base—a finite difference solution, Heat Mass Transfer 31 (1996) 127–135.

[19] C. Balaji, S.P. Venkateshan, Combined conduction, convection and radiation in a slot, Int. J. Heat Fluid Flow 16 (1995) 139–144.

[20] Rammohan Rao, S.P. Venkateshan, Experimental study of free convection and radiation in horizontal fin arrays, Int. J. Heat Mass Transfer 39 (1996) 779–789.

[21] W.W. Lina, D.J. Leela, Second-law analysis on a pin-array under cross flow, Int. J. Heat Mass Transfer 40 (1997) 1937–1945.

[22] B.M. Abramzon, A simple closed-form solution for evaluation of radiative heat transfer from a rectangular fin array, IEEE Trans. Compon., Pack. Manufact. Technol., Part A 20 (2) (1997) 225–229.

[23] H. Yuncu, G. Anbar, An experimental investigation on performance of fins on a horizontal base in free convection heat transfer, Heat Mass Transfer 33 (1998) 507–514.

[24] Andrea de lieto Vollaro, Stefano Grignaffini, Franco Gugliermetti, Optimum design of vertical rectangular fin arrays, Int. J. Therm. Sci. 38 (1999) 525–529.

[25] Senol Baskaya, Mecit Sivrioglu, Murat Ozek, Parametric study of natural convection heat transfer from horizontal rectangular fin arrays, Int. J. Therm. Sci. 39 (2000) 797–805.

[26] A. Guvenc, H. Yuncu, An experimental investigation on performance of fins on a horizontal base in free convection heat transfer, Heat Mass Transfer 37 (2001) 409–416.

[27] Ching-Hung Chiu, Cha'o-Kuang Chen, Application of Adomian's decomposition procedure to the analysis of convective–radiative fins, ASME J. Heat Transfer 125 (2003) 312–316.

[28] A. Dayan, R. Kushnir, G. Mittelman, A. Ullmann, Laminar free convection underneath a downward facing hot fin array, Int. J. Heat Mass Transfer 47 (2004) 2849–2860.

[29] D. Angirasa, R.L. Mahajan, Natural convection from L-shaped corners with adiabatic and cold isothermal horizontal walls, ASME J. Heat Transfer 115 (1993) 149–157.

[30] G. Lauriat, V. Prasad, Non-Darcian effects on natural convection in a vertical porous enclosure, Int. J. Heat Mass Transfer 32 (1989) 2135–2148.

[31] F.P. Incropera, D.P. Dewitt, Fundamental of Heat and Mass Transfer, fourth ed., John Wiley & Sons, 1996.

[32] P.J. Roache, Computational fluid dynamics, Hermosa, Albuquerque, N.M., 1985.